Effect of recombination process in femtosecond laser-induced modification on Ge crystal*

Jia-Qi Ju(居家奇)[1], Zi-Yao Qin(秦子尧)[1], Ju-Kun Liu(刘聚坤)[1,†], Hong-Wei Zhao(赵宏伟)[1], Yao-Qing Huang(黄耀清)[1], Rong-Rong Hu(胡蓉蓉)[1], and Hua Wu(吴华)[2]

[1] *College of Science, Shanghai Institute of Technology, Shanghai* 201418, *China*
[2] *College of Science, Xi'an Shiyou University, Xi'an* 710065, *China*

(Received 11 June 2020; revised manuscript received 31 July 2020; accepted manuscript online 28 September 2020)

The dynamics of produced excited carriers under the irradiation of Ge crystal is investigated theoretically by using femtosecond laser pulse. A two-temperature model combined with the Drude model is also used to study the nonequilibrium carrier density, carrier and lattice temperatures, and optical properties of the crystal. The properties of the surface plasmon wave when excited are also studied. The influences of non-radiation and radiative recombination process on the photoexcitation of the semiconductor during pulse and the relaxation after the pulse are described in detail. The results show that the effects of Auger recombination on the nonequilibrium carrier density and optical properties of the crystal and the properties of the surface plasmon polariton are great, whereas the effect of radiative recombination is extremely small.

Keywords: two-temperature model, Ge crystal, Auger recombination, radiative recombination, surface plasmon polariton

PACS: 42.70.–a, 42.70.Nq, 64.70.kg, 74.25.Gz **DOI:** 10.1088/1674-1056/abbbe9

1. Introduction

The ultrafast processes of semiconductors irradiated by a femtosecond laser have received the attention of scientists[1–7] because they conduce to the understanding of the light-semiconductor interaction. Thus it becomes possible to control the microgeometry of the surface and create the materials with new physical properties.

The two-temperature model (TTM) is extensively used to predict the spatiotemporal dynamics of carriers, especially the temperature dynamics between carrier and lattice, thereby understanding the dynamics of femtosecond laser-processing semiconductors.[7–11] One- and two-photon absorption, ionization, and recombination process are considered when the carrier dynamics is predicted in the TTM. Several recombinations will happen and play important role in the processing result.

The recombination process is very important for carrier dynamics and energy transfer in semiconductor materials. For example, in solar cells, the nonradiative recombination process greatly reduces the photogenerated carrier concentration, resulting in large voltage loss of solar cells. Therefore, the key to the improving of the open circuit voltage and photoelectric conversion efficiency of the device is to minimize or suppress these non-radiative recombination channels.[12,13] However, the influence of recombination process on carrier dynamics and energy transfer during fs laser-material interaction is rarely studied.

Germanium is an important group-IV semiconducting material and has high carrier mobility. Due to its small bandgap energy, Ge can be optically excited with infrared and near infrared radiation,[14] which has been widely used in optics and electronics, such as mid-infrared photodetector.[15]

In this study, the ultrafast dynamics of carrier density, carrier temperature, and lattice temperature after the femtosecond laser irradiation of the surface of a Ge crystal are studied using the TTM model. The influences of the non- and radiative recombination process on transient carrier density and temperature are observed. We find that Auger recombination greatly affects the nonequilibrium carrier density and temperature, and electron–phonon scattering plays an important role in transferring the energy from carrier to lattice. We also study the influences of Auger and radiative recombination process on the other optical parameters of the material and the properties of the surface plasmon polariton (SPP) induced by carrier excitation. The results indicate that the carrier concentration is greatly affected by Auger recombination during the femtosecond laser irradiation of the material. By contrast, the effects of radiative recombination can be neglected.

2. Model

When an fs laser pulse is incident on the Ge surface, the electrons absorb the laser energy through one-photon absorption. The excited electrons are thermalized in several tens of femtoseconds due to the strong electron–electron scattering. The electron temperature rises rapidly and the lattice remains cool. The non-equilibrium system composed of hot electrons

*Project supported by the Young Scientists Fund of the National Natural Science Foundation of China (Grant No. 11804227).
†Corresponding author. E-mail: liujukun@126.com
© 2020 Chinese Physical Society and IOP Publishing Ltd

and cold lattice an be described by the TTM.[7–9] The spatiotemporal dynamics of the carrier density, carrier, and lattice temperature can be calculated using the TTM.

The two-temperature equations are solved by one-dimensional finite difference method under the following conditions: the thickness in the Z direction is $d = 100$ nm, the direction of the incident light is parallel to the Z direction, the laser wavelength is 800 nm, and the laser pulse shape is considered as a Gaussian pulse with a duration of $\tau_p = 50$ fs.

2.1. Carrier dynamics

The electrons are excited from the valence band to the conduction band through one photon absorption in several femtoseconds when the Ge crystal is irradiated by the femtosecond laser pulse. The two-photon absorption process can be ignored in this case because the single photon energy (1.55 eV) is far greater than the band gap of Ge ($E_g = 0.67$ eV) at room temperature,[16] and the same number of holes in the valence band is produced after the electrons have been excited. Several electron–hole pairs are recombined as the excited electrons and holes evolve. The process can be divided into radiative recombination and nonradiative recombination. An electron and a hole will combine and excess carrier energy is radiated in the form of a photon during radiative recombination. This phenomenon is the inverse of the optical excitation process. So, the carrier density will decrease. Non-radiative recombination process includes Auger recombination and carrier–phonon scattering process. During Auger recombination, an electron and a hole recombine, and the excess energy excites another electron to the higher conduction band.[17] In a carrier–phonon scattering process, the carrier energy will decrease due to spontaneous phonon emission, which transfers energy to the lattice. The carriers either in the same conduction or in the valence band valley transfer to a different valley. The carrier–phonon scattering does not change the carrier density.[18] Therefore, the radiative and Auger recombination reduce the carrier density but the carrier–phonon scattering does not change the carrier density. The dynamics of the carrier density can be expressed as follows:

$$\frac{\partial N_e}{\partial t} = D_0 \frac{\partial}{\partial x}\left(\frac{\partial N_e}{\partial x}\right) - \gamma_R N_e^2 - \gamma_A N_e^3 + \frac{\alpha I}{\hbar\omega}, \tag{1}$$

where N_e is the density of free electrons; the first term on the right-hand side describes the carrier transport caused by diffusion; D_0 is the diffusion coefficient; the second term and the third term refer to the radiative recombination with the coefficient γ_R and Auger recombination with the coefficient γ_A, respectively; the last term refers to the single photon absorption. α and $\hbar\omega$ are the single photon absorption coefficient and the energy of the absorbed photons, respectively. The ambipolar diffusion coefficient D_0 can be expressed as follows:[9,19,20]

$$D_0 = \frac{2k_B T_e \mu_h \mu_e}{q(\mu_e + \mu_h)}, \tag{2}$$

where $\mu_e = 3800$ cm^2/(V·s) and $\mu_h = 1800$ cm^2/(V·s) are the electron and hole mobilities,[21] respectively; k_B, T_e, and q are the Boltzmann constant, electron temperature, and electron charge, respectively.

Based on the Beer–Lambert law, the laser intensity at different depths can be written as follows:[22]

$$I(x,t) = \frac{1-R}{t_p} F \exp\left(-\int_0^x (\alpha + \theta N_e)\,\mathrm{d}x\right) \times \exp\left(-2.773\frac{(t - f t_p)^2}{t_p^2}\right), \tag{3}$$

where R is the surface reflectivity of Ge, F is the laser fluence, t_p is the laser pulse width, α is the single-photon absorption coefficient of Ge crystal at 800 nm, θ is the free carrier absorption coefficient, and N_e is the carrier density.

2.2. Optical properties

The optical properties of Ge, such as complex refractive index, absorption coefficient, and reflectivity, are derived from the carrier density through the dielectric permittivity of laser-excited Ge, which can be described by using the Drude model.[23] Further, the other two physics effects are the state and the band filling and band gap renormalization that should be considered for the change of the dielectric permittivity of laser-excited Ge.[24,25] Therefore, the dielectric constant of the excited Ge can be expressed as follows:

$$\tilde{\varepsilon} = \varepsilon - (\varepsilon - 1)N_{eh}/N_c - \left[\omega_p^2/(\omega^2 + \mathrm{i}\omega/\tau)\right], \tag{4}$$

where ε, ω, τ, and ω_p are the dielectric constant of the unexcited crystal Ge, the angular frequency of the incident light, the electron collision time, and the plasma frequency, respectively. The dielectric constant of non-excited Ge at $\lambda = 800$ nm wavelength is $\varepsilon = 22.08 + \mathrm{i}3.03$,[26] and $N_c = 1.8 \times 10^{23}$ cm^{-3} is the number density of valence electrons of Ge crystal. The second term on the right-hand side is derived from the state and the band filling and band gap renormalization. The last term is from the Drude model. The plasma frequency ω_p can be written as[23]

$$\omega_p = \sqrt{e^2 N_e/(\varepsilon_0 m_{opt}^* m_e)}, \tag{5}$$

where ε_0, e, m_e, N_e, and m_{opt}^* are the permittivity of vacuum, electron charge, electron mass, carrier density, and the effective optical mass of carriers, respectively. The real refractive index n and extinction coefficient k can be given by

$$n = \sqrt{(\sqrt{\varepsilon'^2 + \varepsilon''^2} + \varepsilon')/2}, \tag{6}$$

$$k = \sqrt{(\sqrt{\varepsilon'^2 + \varepsilon''^2} - \varepsilon')/2}. \quad (7)$$

The absorption coefficient α and normal-incidence reflectivity R can now be written as

$$\alpha = 4\pi k/\lambda, \quad (8)$$

$$R = \frac{(n-1)^2 + k^2}{(n+1)^2 + k^2}, \quad (9)$$

where λ is the light wavelength in the vacuum.

2.3. Carrier temperature

With the laser pulse irradiating the Ge crystal, carriers are primarily heated through single-photon absorption and free carrier absorption. Free carriers will lose their energy due to spontaneous phonon emission in carrier–phonon scattering process, which transfers energy to the lattice. The Auger recombination does not bring additional energy to the free carrier system. Thus, the carrier temperature can be expressed as follows:[7,9,27]

$$C_e \frac{\partial T_e}{\partial t} = \kappa_e \frac{\partial}{\partial x}\left(\frac{\partial T_e}{\partial x}\right) - \frac{3N_e k_B}{\tau_{ep}}(T_e - T_l) + (\alpha + N_e\theta) I(x,t), \quad (10)$$

where T_e and T_l are the carrier temperature and lattice temperature, and C_e and K_e are the carrier heat capacity and conductivity, respectively. The first two terms on the right-hand side of Eq. (9) are the rate of energy loss due to the ambipolar energy current and the rate of energy exchange between the carriers and lattice, respectively. The last term denotes the laser heat source that heats the carrier through one-photon absorption and free carrier absorption.

2.4. Phonon temperature

The lattice temperature is heated through the carrier-phonon collision, in which the carrier transfers the energy to the phonon. The lattice thermal conductivity of semiconductor material is comparable to the bulk value; therefore, and the thermal transfer in the lattice should be incorporated into the heat conduction equation. Thus,

$$C_l \frac{\partial T_l}{\partial t} = \kappa_l \frac{\partial}{\partial x}\left(\frac{\partial T_l}{\partial x}\right) + \frac{3N_e k_B}{\tau_{ep}}(T_e - T_l), \quad (11)$$

where C_l and K_l are the lattice heat capacity and conductivity, respectively.[27]

The parameters are listed in Table 1.[26,28–32] The specific heat capacity of the free electron is $C_e = 3k_B N_e$. The three equations are numerically solved using the finite difference method. Moreover, the initial Ge carrier density is set to be 5×10^{18} cm^{-3}.[20] In the theoretical calculation, the laser pulse has a full width at half maximum of 50 fs.

Table 1. Parameters of Ge crystal at 800-nm light.

Symbol	Description	Value	Ref.
D_0/cm^2·s^{-1}	ambipolar diffusion coefficient	$2.1\times10^5 T_e$	
γ_R/cm^3·s^{-1}	radiative recombination coefficient	1×10^{-9}	[28]
γ_A/cm^6·s^{-1}	Auger recombination coefficient	2×10^{-31}	[29]
θ/m^2	free carrier absorption coefficient	5×10^{-22}	[30]
τ_{ep}/fs	electron–phonon relaxation time	300	[31]
C_e/J·m^{-3}·K^{-1}	electron heat capacity	$3N_e k_B$	
C_l/J·m^{-3}·K^{-1}	lattice heat capacity	$1.7\times(1+T_l/6000)$	[32]
κ_e/eV·s^{-1}·m^{-1}·K^{-1}	electron thermal conductivity	$-3.58\times10^{19}+6.49\times10^{16}T_e$	[32]
κ_l/W·m^{-1}·K^{-1}	lattice thermal conductivity	$675\times T_l^{-1.23}$	[32]
τ_D/fs	Drude damping time	1	[30]
m^*_{opt}	effective optical mass of carriers	0.22	[32]
ε	unexcited dielectric constant	$22.08+i3.03$	[26]
E_g/eV	band gap	$0.803-3.9\times10^{-4}T_l$	[32]

3. Numerical results and discussion

3.1. Effects of Auger and radiative recombinations

The following three situations are considered to understand the influences of the recombinations: (i) with no Auger recombination, $\gamma_A = 0$; (ii) with no radiative recombination, $\gamma_R = 0$; and (iii) with Auger and radiative recombinations; at $\gamma_A \neq 0$ and $\gamma_R \neq 0$. Figure 1(a) shows the dynamic behaviors of the carrier density on the Ge surface irradiated by 50 fs laser pulse with a laser fluence of 0.1 J/cm^2 in different situations. The profile of the incident femtosecond laser pulse is shown in this figure with a peak of about 242 fs. The high-density carriers are excited from the valence band to the conduction band in all the situations because of the one-photon absorption. The carrier density reaches its peak value of about 2.62×10^{22} cm^{-3} in 252 fs when considering the situation with the Auger and radiative recombinations. The rapid decrease of the carrier density is primarily due to the Auger and radiative recombination process according to Eq. (1). Similarly, the carrier density reaches a slightly higher peak value of 2.74×10^{22} cm^{-3} in 252 fs for the $\gamma_R = 0$ situation. However, the carrier density is 4.95×10^{22} cm^{-3} in 257 fs for the

$\gamma_A = 0$ situation, which is almost twice as much as that of the γ_A situastion and also that of $\gamma_R \neq 0$ situation. This finding shows that the Auger recombination remarkably increases the carrier density. Figure 1(b) shows that the carrier temperature reaches its peak value of 2.65×10^4 in the $\gamma_R = 0$ situation and 2.62×10^4 K in the $\gamma_A \neq 0$ and $\gamma_R \neq 0$ situation, respectively. The tendency of the $\gamma_R = 0$ situation almost coincides with that in the $\gamma_A \neq 0$ situation and in the $\gamma_R \neq 0$ situation. However, in the $\gamma_A = 0$ situation there is observed a much smaller peak value of approximately 1.28×10^4 K. This result means that the Auger recombination greatly affects the carrier temperature in the nonequilibrium state. The comparison among the results of $\gamma_A = 0$ situation, $\gamma_A \neq 0$ situation, and $\gamma_R \neq 0$ situation demonstartes that the transferred energy during the Auger recombination and the carrier density greatly affect the carrier temperature in the nonequilibrium state.

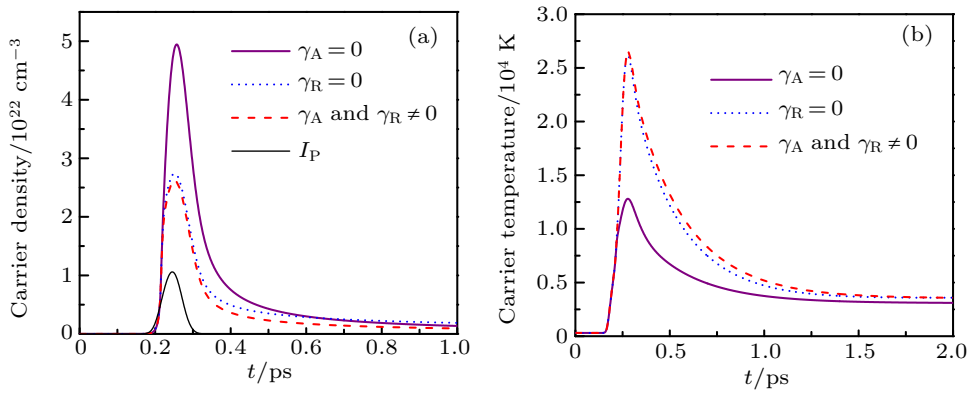


Fig. 1. Time-dependent dynamic behaviors of (a) carrier density and (b) carrier temperature on surface of Ge sample irradiated by 50-fs laser pulse of $F = 0.1$ J/cm^2 for different situations with I_p representing laser pulse.

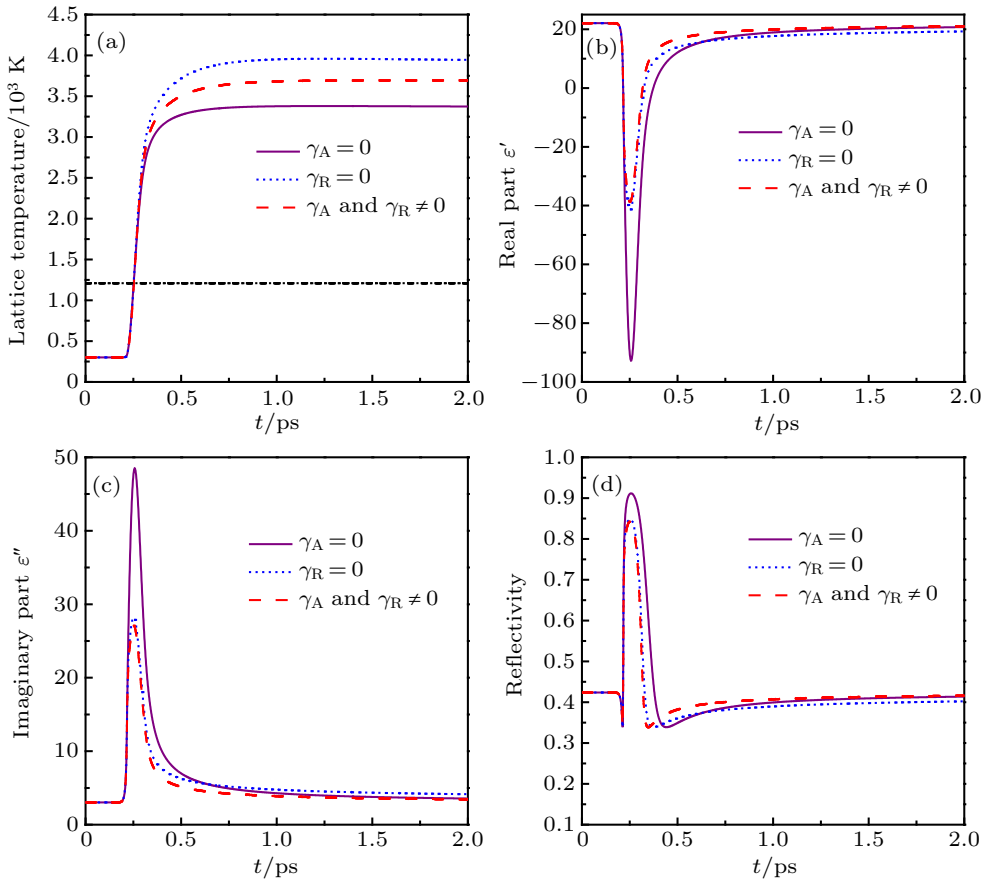


Fig. 2. Evolutions of (a) lattice temperature, (b) real part, and (c) imaginary part of dielectric constant, and (d) reflectivity on Ge surface, with black dash line in panel (a) denoting melting temperature.

Figure 2(a) shows the ultrafast dynamic behaviors of the carrier temperature in different situations. The results show that the tendencies in different situations are almost the same. The lattice temperature increases rapidly to 3.7×10^3 K because of the electron–phonon scattering. The melting temperature of Ge is about 1210 K. The lattice temperature exceeds the melting point greatly. The equilibrium lattice temperatures in the $\gamma_A \neq 0$ and $\gamma_R \neq 0$ situations are larger than that in the

$\gamma_A = 0$ situation but smaller than that in the $\gamma_R = 0$ situation. The results demonstrate that the Auger recombination promotes the heat transfer to the lattice, but radiative recombination does not because the energy produced during the recombination is radiated through photon emission.[18] Figure 2(b) shows the evolution of the real part of the dielectric constant. The minimum value in the $\gamma_A = 0$ situation is smaller than that in the $\gamma_R = 0$, $\gamma_A \neq 0$, and $\gamma_R \neq 0$ situations, separately because the electric constant is related to the carrier density according to Eqs. (4) and (5) and the nonequilibrium carrier density in the $\gamma_A = 0$ situation is the largest in the three situations as shown in Fig. 1(a). The same reason for the imaginary part of the dielectric constant is shown in Fig. 2(c), where the transient value reaches 48.5 in 257 fs. Figure 2(d) indicates the dynamic behavior of the reflectivity on the Ge surface. Reflectivity values initially decrease with carrier density increasing during the pulse duration in the different situations. Then, the values ascend rapidly to the peaks of 0.91, 0.85, and 0.84 in the $\gamma_A = 0$, $\gamma_R = 0$, and $\gamma_A \neq 0$, and $\gamma_R \neq 0$ situations, respectively. Afterwards, reflectivity values decrease and then gradually increase to their initial values.

We further assess how irradiation recombination and the Auger recombination alter carrier density, carrier temperature, and lattice temperature. The maximum carrier density, carrier temperature, and lattice temperature vary at different laser fluences as presented in Fig. 3. The nonequilibrium carrier densities in the $\gamma_A = 0$ situation are very different from those in the $\gamma_A = 0$, $\gamma_R \neq 0$, and $\gamma_A \neq 0$ situations in Fig. 3(a). The divergence among the $\gamma_A = 0$ and $\gamma_R \neq 0$, and $\gamma_A \neq 0$ situations becomes larger with laser fluence increasing. The maximum carrier density in the $\gamma_A = 0$ situation is about twice as much as that in the $\gamma_R \neq 0$ and $\gamma_A \neq 0$ situations at a laser fluence of 0.6 J/cm^2. This finding indicates that the effect of Auger recombination on carrier density becomes greater with fluence increasing. However, the maximum carrier density in the $\gamma_R \neq 0$ and $\gamma_A \neq 0$ situations is almost equal to those in the $\gamma_R = 0$ situation for all laser fluences. Figure 3(b) shows that the Auger recombination greatly changes the maximum carrier temperature with the increase of laser fluence. The maximum nonequilibrium carrier temperatures in the $\gamma_R \neq 0$ and $\gamma_A \neq 0$ situations are larger than that in the $\gamma_A = 0$ situation, because the Auger recombination transfers the energy to the carrier as shown in the comparison of the cases for $\gamma_A = 0$, $\gamma_R \neq 0$, and $\gamma_A \neq 0$ situations in Fig. 1(b). However, the radiative recombination almost does not affect carrier temperature compared with the Auger recombination. Figure 3(c) shows that the lattice temperatures in all the three situations increase with laser fluence increasing. No difference among the $\gamma_A = 0$, $\gamma_R \neq 0$, and $\gamma_A \neq 0$ situations is observed at low fluence. However, the difference is enlarged with laser fluence increasing and rises to 1450 K at 0.6 J/cm^2. The lattice temperature in the $\gamma_A = 0$ situation is smaller than in the $\gamma_R \neq 0$ and $\gamma_A \neq 0$ situations as shown in Fig. 1(b).

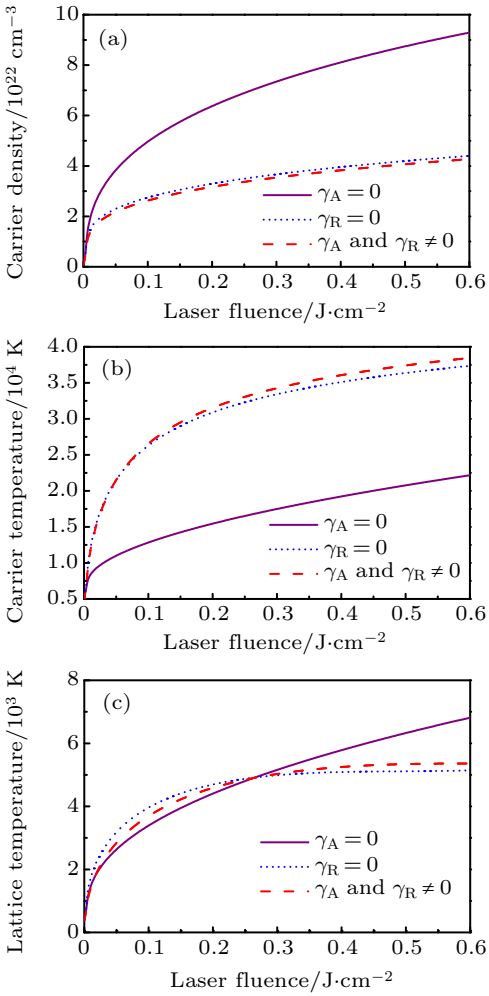


Fig. 3. Laser fluence-dependent (a) maximum carrier density , (b) carrier temperature, and (c) lattice temperature on surface of a 100-nm-thick Ge sample heated by 50-fs laser pulse for $\gamma_R = 0$, and γ_A and $\gamma_R \neq 0$.

3.2. Influence of electron–phonon scattering

The initial transient two-temperature system of hot carrier and cold lattice is formed after being irraduated by fs laser pulse, and the cold lattice thermalizes through electron–phonon scattering as time evolves.[33] In order to evaluate the influence of the electron–phonon scattering, the simulations are carried out with other two different electron–phonon relaxing times. Figure 4 shows the time evolution of electron and lattice temperature with the three different electron–phonon relaxation times. The time taken for electrons and the lattice to reach thermal equilibrium is about 1.6 ps for $\tau_{ep} = 300$ fs, 3.0 ps for $\tau_{ep} = 500$ fs, and 5.0 ps for $\tau_{ep} = 800$ fs, as shown in Fig. 4. Once electron–lattice thermal equilibrium is reached, the calculated maximum surface lattice temperature is about 3600 K for $\tau_{ep} = 300$ fs, 3000 K for $\tau_{ep} = 300$ fs, and 2400 K

for $\tau_{ep} = 800$ fs, separately. The difference in lattice temperature on the surface is due to the difference in electron–phonon relax time. More energy will be transferred from the hot electrons to the lattice for small relaxing time. Consequently, the electron–phonon scattering plays an important role in transferring the energy from carrier to lattice.

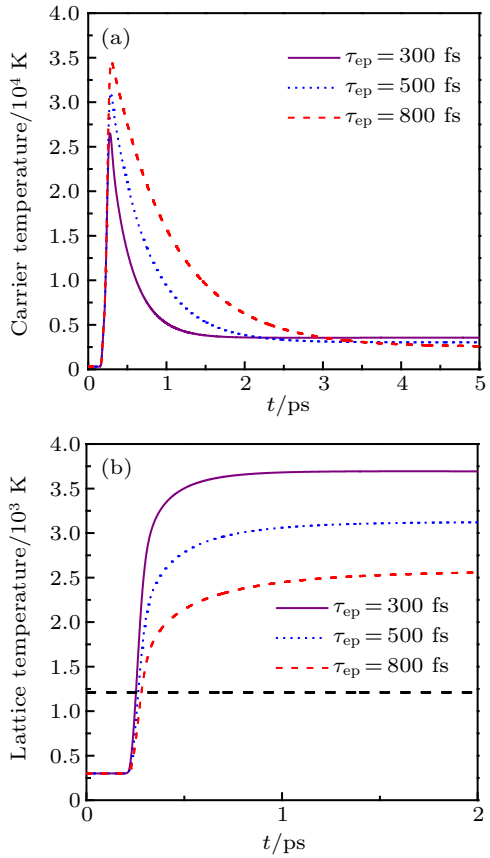


Fig. 4. Calculated time evolutions of (a) surface electron and (b) lattice temperature for different electron–phonon relaxation times, with black dash line in panel (b) representing melting temperature.

3.3. Dielectric constant

The optical properties of Ge are determined by the carrier density through the dielectric permittivity of laser-excited Ge. Massive carriers are excited when the fs laser irradiates the surface of Ge crystal, and the dielectric constant can be described by using the Drude model.[23] The other two physical effects are the state, renormalization, and the band filling and band gap renormalization which are considered for the change of the dielectric permittivity of laser-excited Ge.[24,25] In order to evaluate the two effects, the calculations are performed with and without considering the state renormalization and the band filling and band gap renormalization. Figure 5(a) shows the relationship between the two situations. The divergence between the real parts of dielectric constant under the two situations is about 1.7 at a carrier density of 1.5×10^{22} cm^{-3}. Figures 5(b) and 5(c) show the evolutions of the real and imaginary part of dielectric constant in the two situations. The results show that the difference is small in the cases with and without considering the state renormalization and the band filling and band gap renormalization.

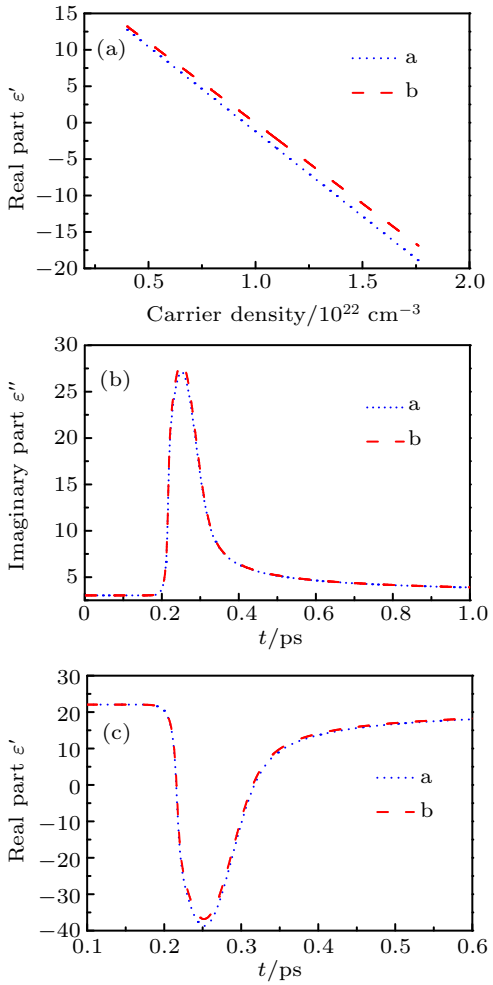


Fig. 5. Calculated relationship between (a) carrier density and real part of dielectric constant, and time evolutions of (b) imaginary part and (c) real part, with a denoting Drude model, and b referring to Drude model with the effect of state renormalization and band filling and band gap renormalization considered.

3.4. SP excitation

Massive carriers can be excited when an fs laser irradiates the crystal, thus leading the optical properties of crystal to change from semiconductor's optical properties to metal's optical properties. The fs laser beam scattered by surface nanoparticles gives rise to phase matching to SPPs. These ensure that the SPPs can be generated at the interface between the crystal and medium. The SPPs interfere with the incident laser beam, causing the optical intensity to be modulated spatially. The spatially varying ablation results in the formation of periodic surface structures.[34–36] The period of the nanostructure is consistent with the SPP wavelength. The wavelength can be written as

$$\lambda_s = \lambda \cdot \mathrm{Re}(\sqrt{(\tilde{\varepsilon} + \varepsilon_d)/(\tilde{\varepsilon}\varepsilon_d)}), \tag{12}$$

where $\lambda = 800$ nm is the wavelength of the incident light, and $\varepsilon_d = 1$ is the dielectric constant of air. The relationship between SP wavelength and carrier density can be obtained

through Eqs. (4), (5), and (11) as shown in Fig. 6(a). The large carrier density of 1.05×10^{22} cm^{-3} is needed for the SP excitation, because the condition of the real part of the dielectric constant is below -1. Furthermore, the relationship between SP wavelength and laser fluence can be obtained and shown in Fig. 6(b). The SP wavelengths in the three different situations increase with laser fluence increasing. The final SP wavelength in the $\gamma_A = 0$ situation is quite different from in the other two situations.

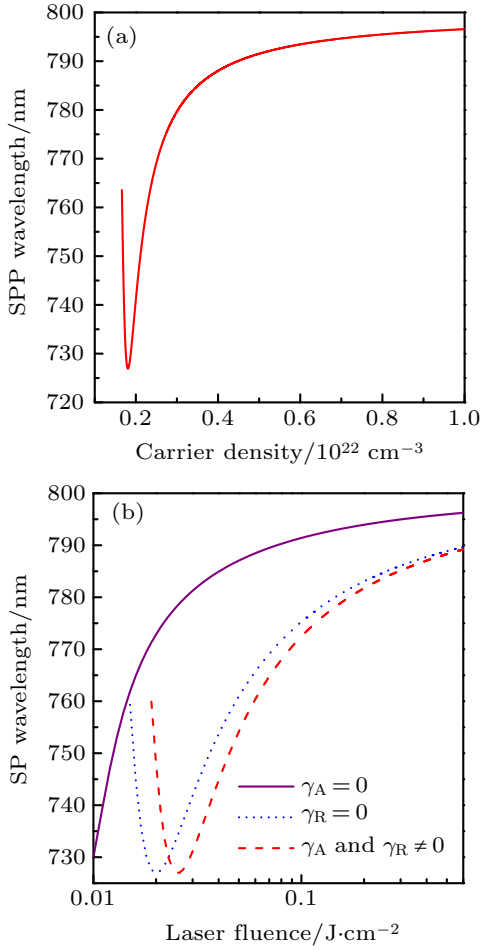


Fig. 6. SP wavelength *versus* (a) carrier density and (b) laser fluence.

Other parameters, such as the damping length along the surface and the decay length away from the surface, are compared except SP wavelength. The SP wave propagation length L_s along the surface can be calculated from

$$L_s = \left(2\omega/c\,\mathrm{Im}\left(\sqrt{(\tilde{\varepsilon}\varepsilon_d)/(\tilde{\varepsilon}+\varepsilon_d)}\right)\right)^{-1}, \tag{13}$$

where ω is the circular frequency of the incident light.[37] The results are shown in Fig. 7(a). The trends in the different situations are the same according to Fig. 6(b), and the conclusion can be easily obtained from Eqs. (11) and (12). The values of SP wave propagation length L_s in the different situations range from about 230 nm to 255 nm. The decay of SP wave away from the surface of the material can be calculated from

$$L_d = \lambda/(2\pi)\sqrt{\varepsilon'^2/(\varepsilon'+\varepsilon_d)}, \tag{14}$$

where ε' is the real part of the dielectric constant of the excited crystal.[37] Figure 7(b) shows that the SP decay lengths decrease with laser fluence increasing in the three situations. The decay length of the SP wave decreases from 63 nm to 20 nm for each of the $\gamma_R = 0$, $\gamma_R \neq 0$, and $\gamma_A \neq 0$ situations and decreases from 62 nm to 10 nm for the $\gamma_A = 0$ situation with laser fluence increasing from 0.1 J/cm^2 to 0.6 J/cm^2.

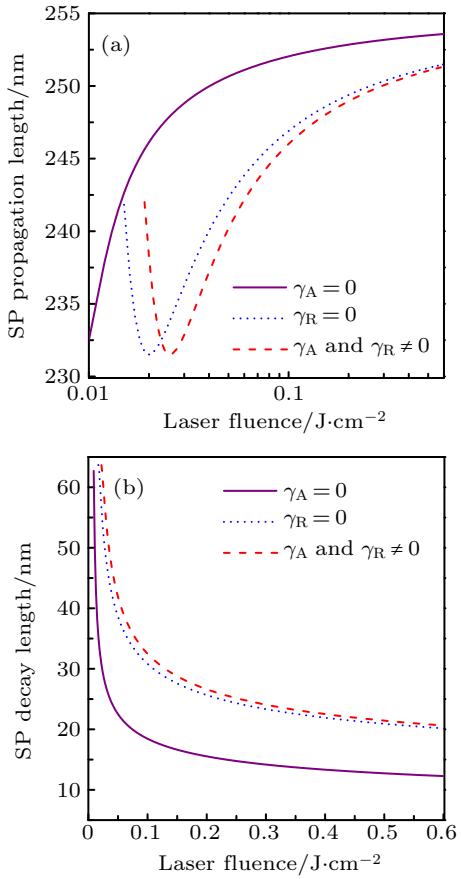


Fig. 7. SP propagation length (a) parallel and (b) perpendicular to surface *versus* laser fluence.

These results show that the three different conditions have similar tendencies when laser fluence inceases. The excitation of SP wave is related to carrier density, and the properties of the SP wavelength in the $\gamma_A = 0$ situation are quite different from those in the other two situations. These findings demonstrate that the influences of Auger and radiative recombinations are weak during laser irradiation.

4. Conclusions

The ultrafast dynamic behaviors of carrier density, carrier temperature, and lattice temperature after the femtosecond laser irradiating the surface of a Ge crystal are studied by the TTM-Drude model. We find that Auger recombination greatly affects the transient carrier density and temperature, *i.e.* the concentration of transient carriers decreases to a half, but the carrier temperature is doubled due to Auger recombination. However, radiation recombination has little effect on carrier

density or temperature. We also study the influences of the Auger and radiation recombination process on other optical parameters of the material andfind that the former greatly influences the dielectric constant, which is related to the carrier density. Finally, we study the excited SP and find that Auger recombination greatly affects the SP properties. Overall, our results indicate that the carrier concentration and temperature are greatly affected by Auger recombination during the femtosecond laser reacting with the material. By contrast, the effect of the radiative recombination can be neglected.

References

[1] Garcial-Lechuga M, Puerto D, Fuentes-Edfuf Y, Solis J and Siegel J 2016 *ACS. Photon.* **3** 1961

[2] Murphy R D, Torralva B, Adams D P and Yalisove S M 2013 *Appl. Phys. Lett.* **103** 141104

[3] Kafka K R P, Austin D R, Li H, Yi A Y, Cheng J and Chowdhury E A 2015 *Opt. Express* **23** 19432

[4] Jia X, Yuan Y, Yang D, Jia T and Sun Z 2014 *Chin. Opt. Lett.* **12** 113203

[5] Jia X, Jia T Q, Peng N, Feng D H, Zhang S A and Sun Z R 2014 *J. Appl. Phys.* **115** 143102

[6] Cheng K, Liu J, Cao K, Chen L, Zhang Y, Jiang Q, Feng D, Zhang S, Sun Z and Jia T 2018 *Phys. Rev. B* **9** 184106

[7] Liu J, Jia X, Wu W, Cheng K, Feng D, Zhang S, Sun Z and Jia T 2018 *Opt. Express* **26** 6302

[8] Yang M, Wu Q, Chen Z, Zhang B, Tang B, Yao J, Drevensek-Olenik I and Xu J 2014 *Opt. Lett.* **39** 343

[9] Liu J, Zhao H, Cheng K, Ju J, Feng D, Zhang S, Sun Z and Jia T 2019 *Opt. Express* **27** 37859

[10] Margiolakis A, Tsibidis G D, Dani K M and Tsironis G P 2018 *Phys. Rev. B* **98** 224103

[11] Petrakakis E, Tsibidis G D and Stratakis E 2019 *Phys. Rev. B* **99** 195201

[12] Polman A, Knight M W, Garnett E C, Ehrler B and Sinke W C 2016 *Science* **352** 4424

[13] Luo D, Su R, Zhang W, Gong Q and Zhu R 2020 *Nat. Rev. Mater.* **5** 44

[14] Seo D, Gregory J M, Feldman L C, Tolk N H and Cohen P I 2011 *Phys. Rev. B* **83** 195203

[15] Zhu J, Zhu H, Xu H, Weng Z and Wu H 2018 *Infrared Physics & Technology* **92** 13

[16] Cavalleri A, Siders C W, Rose-Petruck C, Jimenez R, Tóth C, Squier J A, Barty C P J, Wilson K R, Sokolowski-Tinten K, Horn von Hoegen M and von der Linde D 2001 *Phys. Rev. B* **63** 193306

[17] Fu J, Xu Q, Han G, Wu B and Sum T C 2018 *Nat. Commun.* **8** 1300

[18] Sundaram S K and Mazur E 2002 *Nat. Mater.* **1** 217

[19] Agassi D 1984 *J. Appl. Phys.* **55** 4376

[20] Zollner S, Myers K D, Dolan J M, Bailey D W and Stanton C J 1998 *Thin Solid Films* **313** 568

[21] Prince M B 1953 *Phys. Rev.* **92** 681

[22] Jiang L and Tsai H L 2005 *Journal of Heat Transfer* **127** 1167

[23] Liu J, Jia T, Zhao H and Huang Y 2016 *J Phys. D: Appl. Phys.* **49** 435105

[24] Sokolowski-Tinten K and Von d L D 2000 *Phys. Rev. B* **61** 2643

[25] Wang L, Xu, B B, Cao X W, Li Q K and Sun H B 2017 *Optica* **4** 637

[26] Aspnes D E and Studna A A 1983 *Phys. Rev. B* **27** 985

[27] Tsibidis G D, Barberoglou M, Loukakos P A, Stratakis E and Fotakis C 2012 *Phys. Rev. B* **86** 115316

[28] Carroll L, Friedli P, Neuenschwander S, Sigg H, Cecchi S, Isa F and Faist J 2012 *Phys. Rev. Lett.* **109** 057402

[29] Auston D H, Shank C V and LeFur P 1975 *Phys. Rev. Lett.* **35** 1022

[30] Alfano R R 1984 *Semiconductors probed by ultrafast laser spectroscopy* (Academic Press) p. 87

[31] Yeh T T, Shirai H, Tu C M, Fuji T, Kobayashi T and Luo C W 2017 *Sci. Rep.* **7** 40492

[32] Chen J K, Tzou D Y and Beraun J E 2005 *Int. J. Heat Mass Transfer* **48** 501

[33] Hwang T Y, Vorobyev A Y and Guo C 2009 *Appl. Phys. Lett.* **95** 123111

[34] Das S K, Messaoudi H, Debroy A, McGlynn E and Grunwald R 2013 *Opt. Mater. Express* **3** 1705

[35] Huang M, Zhao F, Cheng Y, Xu N and Xu Z 2009 *ACS Nano* **3** 4062

[36] Wang Y L, Zhao B, Min C J, Zhang Y Q, Yang J J, Guo C L and Yuan X C 2020 *Chin. Phys. B* **29** 027302

[37] Raether H 1988 *Surface plasmons on smooth and rough surfaces and on gratings* (Berlin: Springer-Verlag) p. 209